

Antiferromagnetic interlayer exchange coupling in all-semiconducting EuS/PbS/EuS trilayers

C. J. P. Smits,* A. T. Filip, H. J. M. Swagten, B. Koopmans, and W. J. M. de Jonge
*Department of Applied Physics, Center for NanoMaterials and COBRA Research Institute, Eindhoven University of Technology,
 P.O. Box 513, 5600 MB, Eindhoven, The Netherlands*

M. Chernyshova, L. Kowalczyk, K. Graszka, A. Szczerbakow, and T. Story
Institute of Physics, Polish Academy of Sciences, Al. Lotników 32/46, 02-668 Warszawa, Poland

W. Palosz
BAE/NASA-Marshall Space Flight Center, Huntsville, Alabama 35812, USA

A. Yu. Sipatov
National Technical University KPI, 61002 Kharkov, Ukraine

(Received 1 December 2003; revised manuscript received 20 April 2004; published 23 June 2004)

A comprehensive experimental study on the antiferromagnetic interlayer exchange coupling in high quality epitaxial all-semiconducting EuS/PbS/EuS trilayers is reported. The influence of substrates, of the thickness of the nonmagnetic PbS spacer layer, and of temperature was investigated by means of SQUID magnetometry. In trilayers with a PbS thickness between 4 and 12 Å the low temperature hysteresis loops showed the signature of antiferromagnetic coupling. The value of the interlayer exchange coupling energy was determined by simulating the data based on a Stoner-Wohlfarth model. An important observation was that the interlayer exchange coupling energy varies strongly with temperature, consistent with a power-law dependence of the exchange coupling constant on the saturation magnetization of the EuS layers. While no theoretical description is readily available, we conjecture that the observed behavior is due to a dependence of the interlayer exchange coupling energy on the exchange splitting of the EuS bands.

DOI: 10.1103/PhysRevB.69.224410

PACS number(s): 75.30.Et, 75.50.Pp, 75.70.Cn

I. INTRODUCTION

Magnetic semiconductors^{1,2} may become crucial components for the further development of the field of spintronics.^{3,4} If magnetic semiconductors are to be used in electronic applications, it is desirable, maybe even necessary, to be able to tune their switching fields. This can in principle be achieved experimentally by exchange coupling the semiconducting ferromagnet to an antiferromagnet,⁵ as is successfully applied for metallic structures,⁶ or, alternatively, by exchange coupling two magnetic semiconductor layers, separated by a nonmagnetic semiconductor layer. In contrast to metallic ferromagnets, where the interlayer exchange coupling is well-studied⁷ and theoretically understood within the Ruderman, Kittel, Kasuya, and Yosida (RKKY) or a quantum interference model,^{8,9} little is known about interlayer coupling between two ferromagnetic semiconductors across a nonmagnetic semiconductor where the carrier concentration is too low to support the RKKY mechanism.^{10,11} Therefore the study of the magnetic interlayer coupling in all-semiconductor structures may not only be technologically relevant,¹ but is also of fundamental interest. It is the aim of this paper to experimentally study the fundamentals of interlayer exchange coupling in all-semiconducting systems.

Presently interlayer exchange coupling in semiconductor systems has been observed for only a limited amount of materials. In EuTe/PbTe/EuTe¹² and MnTe/ZnTe/MnTe¹³ superlattices an antiferromagnetic coupling between the antiferromagnetic EuTe and MnTe layers has been observed, whereas between the ferromagnetic GaMnAs layers in

GaMnAs/GaAs/GaMnAs trilayers only a ferromagnetic interlayer exchange coupling is found.^{14,15} Antiferromagnetic interlayer exchange coupling between ferromagnetic semiconductors was first found in EuS/YbSe/EuS and EuS/PbS/EuS superlattices.^{10,14} The EuS/PbS/EuS system which is the subject of this paper, shows a clear *antiferromagnetic* interlayer exchange coupling between the two *ferromagnetic* EuS layers, as determined from neutron diffraction and magnetometry.¹⁰ Moreover, the magnetic properties of this EuS system have also been the subject of several earlier studies on epitaxial thin EuS films and multilayers.^{16–18} Europium sulfide, EuS, is one of the best-known^{19,20} ferromagnetic semiconductors, and has a Curie temperature of 16.8 K and a band gap of 1.6 eV below T_C .²¹ EuS grows in the rocksalt structure and possesses a cubic in-plane anisotropy with a [110] easy axis. Lead sulfide, PbS, is a narrow-gap nonmagnetic semiconductor, having a band gap of 0.3 eV,²² and is lattice matched with EuS, enabling epitaxial growth of our structures.

With respect to the physical origin of the interlayer exchange coupling in semiconductor systems, several scenarios may be envisioned.²³ In III–V diluted magnetic semiconductor heterostructures the coupling is mediated by the holes in the valence band.^{11,24} Another possible mechanism is the Bloembergen-Rowland indirect exchange via virtual excited states in either the conduction or the valence band of the nonmagnetic quantum well.²⁵ However, both mechanisms are expected to lead to a ferromagnetic coupling, contrary to what is observed experimentally. Interlayer exchange coupling for II–VI semiconductor structures is explained by as-

suming that it is mediated by shallow donor impurities, but these have never been observed in PbS.^{26–28} An antiferromagnetic exchange coupling in EuS/PbS/EuS was obtained theoretically by Blinowski and Kacman, based on a 0 K calculation of the spin-dependent total energy of the valence electrons of the EuS/PbS/EuS structure.²⁹

In this paper we present an experimental study of the antiferromagnetic interlayer exchange coupling in high quality epitaxial EuS/PbS/EuS trilayers. The paper is organized as follows: First the exact structure and quality of the samples used is discussed, and their magnetic behavior is described. Then a Stoner-Wohlfarth-like model is applied in order to extract the interlayer exchange coupling energy and anisotropy from the hysteresis loops. This is followed by the main results of the paper: the analysis of the dependence of the interlayer exchange coupling energy, first, on the thickness of the nonmagnetic PbS spacer and, second, on temperature. The paper ends with a discussion aiming at understanding the temperature dependence by taking into account the effect of the magnetic moment of EuS on the band structure in the trilayer.

II. EXPERIMENT

EuS/PbS/EuS trilayer structures are grown epitaxially by high vacuum evaporation of EuS, employing an electron gun, and PbS using electrically heated tungsten boats. Monocrystalline KCl and PbS substrates with freshly cleaved (001) surfaces are used.³⁰ The substrate temperature during growth is 250–300 °C. The thickness of the layers is monitored *in situ* with a calibrated quartz resonator, and is also checked by x-ray diffraction analysis after growth. The detailed design of the trilayer structures studied is as follows: PbS (or KCl)(001) substrate/PbS(buffer)/EuS(*t*)-PbS(*d*)-EuS(*t*)/PbS(cap) with a ferromagnetic layer thickness of $t=30\text{--}200$ Å, and a nonmagnetic spacer thickness of $d=4\text{--}90$ Å. The structures include 500–1000 Å thick PbS buffer layers accommodating any substrate-multilayer lattice mismatch strain, as well as 100–700 Å thick PbS cap layers protecting the trilayer against surface oxidation. An x-ray diffraction analysis of the crystal quality of EuS/PbS structures on PbS^{16,30,31} shows that these are monocrystalline (001) crystallographically oriented layers with a rocking curve full width at half maximum of about 0.04°–0.08°. For EuS/PbS superlattice type structures prepared in parallel, the x-ray diffraction spectra show clear superlattice satellite peaks even up to the seventh order, indicating well-defined planar structures of ultrathin magnetic and nonmagnetic layers. Due to the very good lattice match between EuS and PbS these semiconductor materials can be grown as pseudomorphically strained structures up to the total thickness of about 2000 Å. Previous studies have shown that the interdiffusion at the EuS–PbS interface is low and corresponds to an intermixing of only 1–2 monolayers (ML). Therefore, the main morphological defects at the interface are expected to originate from various steps inevitably present, e.g., due to substrate roughness. An atomic force microscopy (AFM) analysis of the freshly cleaved (001) surfaces of KCl and PbS substrate crystals shows flat regions attributed to terraces of

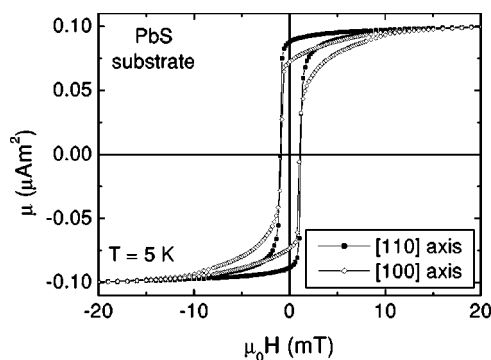


FIG. 1. Hysteresis curves at 5 K measured in-plane along [110] and [100] axes for a EuS(30 Å)/PbS(50 Å)/EuS(30 Å) trilayer grown on a PbS substrate and covered with a PbS capping layer.

the cleaved substrates (root mean square, rms, roughness of 10 Å) for an area of up to $10 \times 10 \mu\text{m}^2$. These regions are separated by few-monolayer high steps. The cleaved surfaces also show larger (0.1 μm) steps but these are located at macroscopically large distances (of the order of 100 μm). AFM analysis of the full EuS/PbS/EuS trilayer structures exposed to air shows a rms surface roughness of about 40 Å (for the area of $10 \times 10 \mu\text{m}^2$) presumably due to surface oxidation of the PbS cap layer.

The magnetic behavior of the EuS/PbS/EuS layers is investigated by SQUID magnetometry. Hysteresis curves as well as the magnetic moment as a function of temperature for different applied fields are measured. In the following section, we discuss how physical information can be extracted from the hysteresis curves.

III. RESULTS AND DISCUSSION

A. Modeling the hysteresis loops

In general, at low temperatures, all samples show a saturation magnetic moment within 10% of the expected moment for an ideal EuS layer ($7 \mu_B/\text{atom}$), confirming the high quality of the samples. A plot of a measurement of a hysteresis curve along a [110] and a [100] axis of two uncoupled EuS layers is depicted in Fig. 1. The rocksalt structure of EuS leads to a cubic in-plane magnetic anisotropy. Indeed, for the loop along the [110] axis the magnetization switches to almost the full saturation value, whereas the magnetic moment measured along the [100] axis switches only to roughly 0.7 times the saturation magnetic moment, corresponding to a moment 45° off the field direction.

Figure 1 also shows that the coercive field of such EuS layers is typically 2 mT. At fields of the order of 10 mT, however, the magnetic moment has not completely reached saturation. We ascribe this to the existence of domains of low formation energy in EuS, an effect that has been known for a long time for EuS, and is supposed to be due to the relatively small exchange interaction in the material.³²

Figure 2 shows hysteresis curves for a EuS(30 Å)/PbS(11 Å)/EuS(30 Å) trilayer. For applied magnetic fields below 2 mT a plateau of low total magnetic moment due to near antiparallel orientation of both EuS layers is visible, a

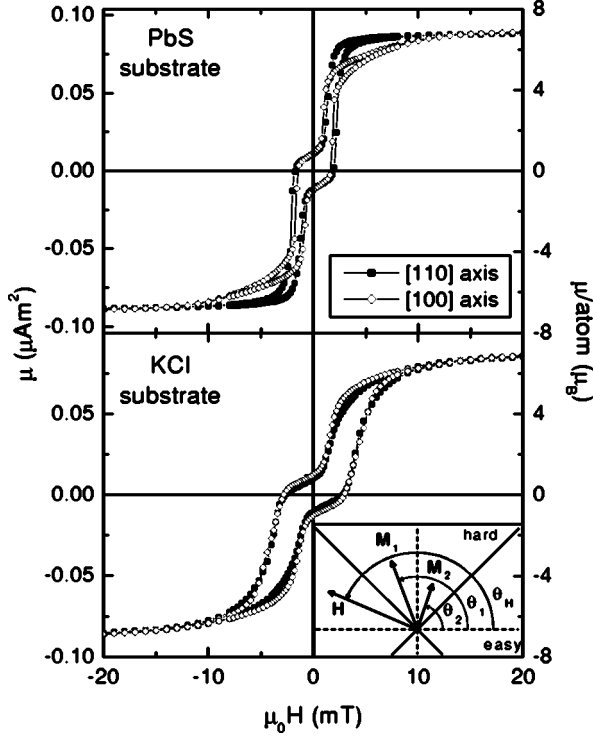


FIG. 2. Hysteresis curves for EuS(30 Å)/PbS(11 Å)/EuS(30 Å) trilayers at 5 K measured in-plane along [110] and [100] axes, grown both on PbS and on KCl substrates covered with a PbS buffer layer. The inset explains the definition of the angles used in Eq. (1).

feature that all (a few dozen) samples with PbS spacers between 6 and 12 Å exhibit. Figure 2 shows that for the layers grown on PbS substrates a clear difference can be observed between measurements with the field along the in-plane [110] and [100] directions, in agreement with the cubic anisotropy of EuS. For EuS layers grown on KCl there is almost no difference in the hysteresis loops measured along [110] and [100] axes. Although the width of the plateau of low magnetic moment is generally larger by a few tens of percents for trilayers on KCl substrates with respect to the same ones grown in parallel on PbS substrates, in this paper we will focus on the trilayers on PbS substrates since the anisotropy is better defined there, and, as a consequence, the switching field between antiparallel and parallel alignment of the EuS layers can be determined more accurately.

Hysteresis loops for different temperatures with the magnetic field along the easy [110] crystal axis are shown in Fig. 3 for a EuS(60 Å)/PbS(6 Å)/EuS(60 Å) sample. The plateau near zero field is identified with the existence of an antiparallel arrangement yielding zero magnetization. Clearly the width of this plateau of antiferromagnetic coupling diminishes with increasing temperature. A detailed discussion of the temperature dependence will be given in Sec. V.

In order to be able to quantify the coupling strength, a simple Stoner-Wohlfarth-like model is used. Within this model, besides the magnetostatic energy and cubic magnetic anisotropy, interlayer coupling between the two magnetic layers is taken into account.³³ We consider two identical,

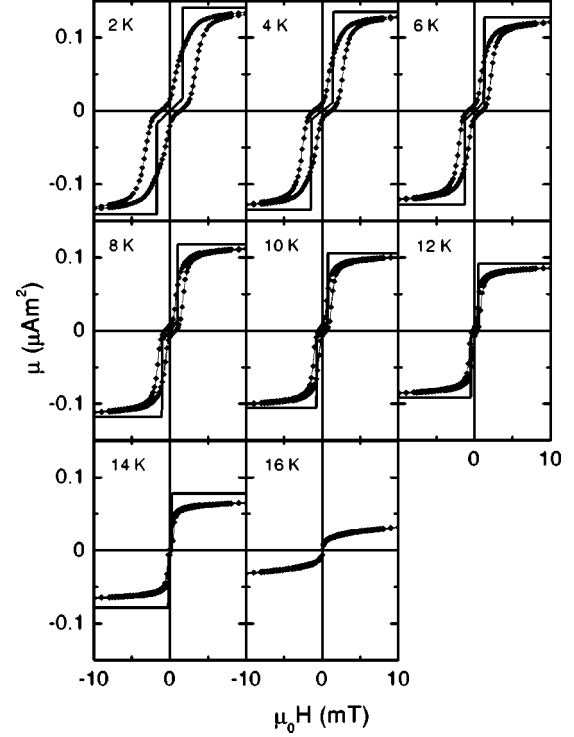


FIG. 3. Easy axis [110] hysteresis loops for a EuS(60 Å)/PbS(6 Å)/EuS(60 Å) trilayer for different temperatures below the Curie temperature. In addition curves simulated using a Stoner-Wohlfarth model are drawn showing a fair qualitative agreement with the experiment in the region of antiferromagnetic coupling.

single-domain layers with a saturation magnetization M , thickness t , and cubic anisotropy. The total magnetic areal energy density E/A of the system is given by

$$\begin{aligned}
 E/A = & -\mu_0 H M t \cos(\vartheta_1 - \vartheta_H) - \mu_0 H M t \cos(\vartheta_2 - \vartheta_H) \\
 & + K_4 t \sin^2 \vartheta_1 \cos^2 \vartheta_1 + K_4 t \sin^2 \vartheta_2 \cos^2 \vartheta_2 \\
 & - J \cos(\vartheta_1 - \vartheta_2),
 \end{aligned} \quad (1)$$

where H is the applied magnetic field, and ϑ_H , ϑ_1 , and ϑ_2 are the angles of the field and the magnetization of each layer with a reference axis (see the inset of Fig. 2). K_4 and J denote the cubic anisotropy per volume unit and the interlayer coupling energy per unit of surface area, respectively. The choice of the reference axis can be used to define the direction of the easy axes.

For a fixed layer thickness, the hysteresis curve is simulated by numerical minimization of the total energy as a function of the magnetization direction of each layer. We chose to simulate the unhysteretic curves, based on the global minimum of the energy, as Stoner-Wohlfarth models generally overestimate coercivities, leading also in this case to unrealistically high switching fields. In the past the same technique has already proven useful in the study of magnetic interlayer coupling in metallic structures.⁷

The simulated curves are also shown as solid lines in Fig. 3. The agreement between simulation and experimental data is reasonably good for low applied magnetic fields. From the

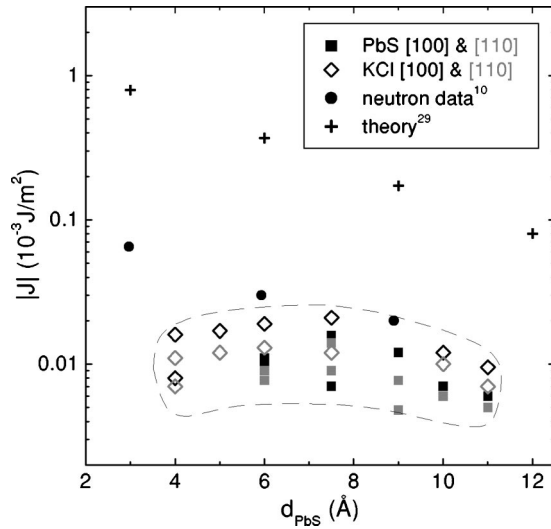


FIG. 4. Overview of the measured antiferromagnetic interlayer exchange coupling energy J as a function of the PbS spacer layer thickness in EuS/PbS/EuS trilayers. Closed squares correspond to samples grown on PbS, open diamonds to those on KCl substrates. Gray corresponds to easy axis measurements and black to those along hard axes. The EuS thickness varied between 30 and 60 Å. The contour is a guide to the eye. For comparison, values from neutron diffraction measurements on EuS/PbS superlattices grown on PbS substrates (Ref. 10) (full circles) as well as the theoretical prediction by Blinowski and Kacman (Ref. 29) (crosses) are also plotted.

calculations it follows that the width of the plateau of antiferromagnetic alignment (i.e., the switching field) is mainly determined by the interlayer exchange coupling, while the zero-field susceptibility (i.e., the slope of the plateau) is mostly determined by the anisotropy energy. Therefore, by fitting the low-field behavior, the interlayer exchange coupling energy J and the crystalline anisotropy K_4 can be determined.³⁴

At higher fields the measured data deviate from the model in the sense that saturation is reached slower than expected. However, this discrepancy is an intrinsic property of the individual EuS layers, as the hysteresis loops for uncoupled layers are similarly curved (Fig. 1). The field at which the transition towards a ferromagnetic alignment of the EuS layers is completed is thus hard to define, again motivating our choice to use the low-field behavior for our simulations.

B. Spacer thickness dependence

One possible route to gain insight into the underlying physics of the interlayer coupling is to consider its dependence on the nonmagnetic spacer thickness. Figure 4 summarizes the results of such an investigation. The data are obtained by simulating the hysteresis loops of several EuS/PbS/EuS trilayers with various spacer thicknesses, using the method described in the previous section. Considering the sign of the interaction to start with, the interlayer exchange coupling is always found to be antiferromagnetic with simulated values of the interlayer exchange coupling energy J of the order of 10^{-3} – 10^{-2} mJ/m² for PbS spacer

thicknesses in the range of 4–11 Å. For thicker spacers we could not observe any interlayer coupling. As mentioned before, the RKKY theory predicts an oscillating interlayer exchange coupling as a function of both the thickness of the nonmagnetic spacer and the local carrier concentration, starting with a ferromagnetic interaction at the lowest carrier concentration and the thinnest spacer layers. For a carrier concentration of 10^{20} cm⁻³ a ferromagnetic coupling is expected for all spacers up to 30 Å.¹¹ Since the carrier concentration in our PbS spacer layer is 10^{18} – 10^{19} cm⁻³, the interlayer coupling should be ferromagnetic for our spacer thicknesses, while we observe antiferromagnetic coupling for spacers as thin as 4 Å thickness. Therefore, we find it reasonable to exclude RKKY as a potential mechanism describing the coupling in EuS/PbS/EuS.

Blinowski and Kacman predicted an antiferromagnetic interlayer exchange coupling based on a calculation of the spin dependent total energy of the valence electrons of the EuS/PbS/EuS structure.²⁹ The observed interlayer exchange coupling is one order of magnitude weaker than predicted within their model (see Fig. 4). However, the model assumed perfectly flat layers with an integer number of atomic monolayers in the spacer layer, whereas for metallic multilayers it has been reported that alloying effects at the interfaces decrease the coupling strength considerably,³⁵ and such an effect could also be present in the case of semiconductors. As can be seen from Fig. 4, the interlayer exchange coupling energy appears to reach a maximum for spacer thicknesses around 2.5 monolayers (7.5 Å). For thicker spacers the measured values are consistent with those found in neutron reflectivity measurements.¹⁰ Moreover, the decrease in the coupling energy with increasing spacer thickness is in qualitative agreement with the calculations of Blinowski and Kacman,²⁹ although any detailed comparison with theory is not possible due to the rather large spread of our data.

For thinner spacer layers (< 7.5 Å) the magnitude of the interlayer exchange coupling energy becomes slightly smaller again, contrary to the neutron reflectivity data. For these low spacer thicknesses, corresponding to 1–2 monolayers of PbS, the existence of pinholes is very likely, potentially causing strong local ferromagnetic interactions between the two magnetic layers. Measurements of the magnetic moment are sensitive to the net moment of the whole sample and therefore do not separate ferromagnetically and antiferromagnetically coupled regions in the trilayer, resulting in an averaged smaller value of the interlayer exchange coupling energy in this regime of thin (< 7.5 Å) spacers. The neutron reflectivity results in Fig. 4 monitor only antiferromagnetic alignment between the magnetic layers in the sample, which is insensitive to the presence of local ferromagnetic coupling.

Summarizing, we observe that the interlayer exchange coupling energy is reduced as the spacer thickness increases in the range above about 7.5 Å, in qualitative agreement with the calculations by Blinowski and Kacman.²⁹ However, for very thin spacer layer thicknesses the net interlayer coupling energy decreases, most probably due to the existence of pinholes in the PbS, resulting in a mix of a strong local ferromagnetic interaction and an antiferromagnetic coupling elsewhere, leading to a smaller average coupling strength.

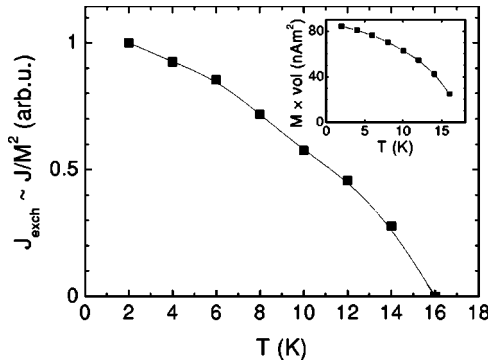


FIG. 5. Antiferromagnetic interlayer exchange coupling constant as a function of temperature for a EuS(60 Å)/PbS(6 Å)/EuS(60 Å) sample. The inset shows the behavior of the saturation magnetization of a single layer as a function of temperature.

C. Temperature dependence

A second route in the investigation of the interlayer exchange coupling in EuS/PbS/EuS trilayers is to study its temperature dependence in a systematic way. If one takes into consideration the microscopic origin, the relevant quantity to study is not the interlayer exchange coupling energy J , but rather the exchange coupling constant J_{exch} , defined as $J = J_{\text{exch}} \sum_{i,j} \mathbf{S}_i \cdot \mathbf{S}_j$. The summation is taken over all spins at the interface between the magnetic layers ($i \in \text{layer 1}$ and $j \in \text{layer 2}$). As the exchange coupling between neighboring spins within the same EuS layer is expected to be much stronger than the exchange coupling across the nonmagnetic layer, the local correlations between spins across layers can be neglected. As a direct consequence the summations over spins can be replaced with the average magnetizations and J_{exch} should be proportional to J/M^2 .

The simplest assumption is that the microscopic coupling is temperature and layer magnetization independent ($J_{\text{exch}} = \text{constant}$). In this case J/M^2 remains constant as a function of temperature. However, recently we concluded (see Chernyshova *et al.*¹⁸) that the interlayer exchange coupling was actually temperature or magnetization dependent. This was inferred from measurements of the temperature dependence of the net magnetic moment in EuS/PbS/EuS trilayers and subsequent qualitative modeling.

The interlayer exchange coupling constant J_{exch} is plotted in Fig. 5 for a EuS(60 Å)/PbS(6 Å)/EuS(60 Å) sample, extracted from the hysteresis curves as shown in Fig. 3. We observe a strong dependence of the interlayer exchange coupling constant on temperature, showing a qualitatively similar behavior as the saturation magnetization of the EuS layers.

To further quantify this, the log-log plot of the antiferromagnetic interlayer exchange coupling constant J_{exch} as a function of the saturation magnetization of the EuS layers is shown in Fig. 6 for three individual samples. For all three samples a clear power law dependence can be observed, with an exponent around 1.8–1.9 for the two samples with a 60 Å thick EuS layer, and a smaller exponent (1.4) for the sample with the thinner (40 Å) EuS layer, suggesting a possible de-

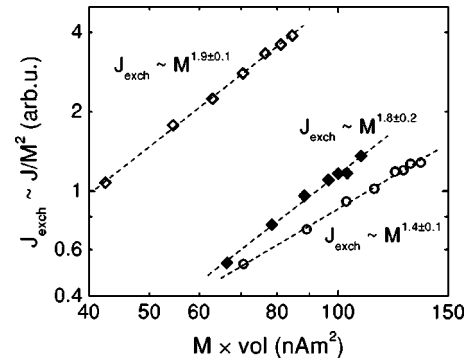


FIG. 6. Antiferromagnetic interlayer exchange coupling constant (coupling energy J divided by M^2) plotted on a double logarithmic scale as a function of the saturation magnetization of the EuS layers for EuS(60 Å)/PbS(6 Å)/EuS(60 Å) (open diamonds), 60 Å/9 Å/60 Å (closed diamonds), and 40 Å/7.5 Å/40 Å (open circles) trilayers. Note the horizontal shift due to different sample areas.

pendence of the coupling constant on the EuS layer thicknesses. However, a more detailed study is needed to draw firm conclusions on this issue. We believe that the power-law behavior on the layer magnetization should be regarded as an intrinsic property of the interlayer coupling mechanism in EuS/PbS/EuS trilayers.

In order to confirm this intrinsic temperature dependence of the interlayer coupling, the net magnetic moment of the trilayer μ was also directly measured as a function of temperature for different applied magnetic fields. A plot is given in Fig. 7 for the same EuS(60 Å)/PbS(6 Å)/EuS(60 Å) sample. For large applied magnetic fields, the magnetization shows a monotonic increase as temperature decreases, consistent with a parallel alignment of the two magnetic layers. In contrast, for lower applied fields, the magnetization shows a sharp decrease in magnitude below a certain temperature, as a consequence of a change from F to AF alignment of the two magnetic layers. A straightforward calculation shows that, if one neglects the anisotropy and assumes the interlayer exchange coupling constant J_{exch} to be temperature independent, the magnetic moment of the sample remains constant below a certain temperature. For finite values of anisotropy, a monotonous increase of the total magnetic moment during cooling is expected for all applied fields. In

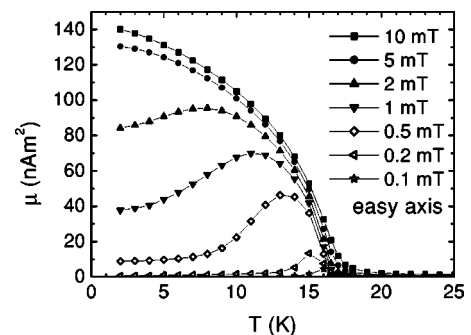


FIG. 7. Temperature dependence of the total magnetic moment of an EuS(60 Å)/PbS(6 Å)/EuS(60 Å) sample for various constant magnetic fields along the [110] easy axis.

contrast, we observe a sharp decrease in the magnetic moment below a certain temperature indicating an intrinsic dependence of the interlayer exchange coupling constant on either temperature or magnetic moment of the layer, which is a straightforward confirmation of our earlier observation.

To the best of our knowledge, the exact physical origin of the AF interlayer exchange coupling in systems like EuS/PbS/EuS is not yet known and theoretical predictions on its temperature dependence are not available. In metallic systems, the interlayer coupling is described within the RKKY model,³⁶ and the temperature dependence of the interlayer exchange coupling constant stems from the broadening of the Fermi-Dirac distribution with increasing temperature. In *p*-type semiconductor systems, the coupling between spins is mediated via the holes in the valence band.¹¹ However, carrier mediated interactions generally lead to a ferromagnetic coupling for our carrier concentrations and spacer layer thicknesses, while we observe an antiferromagnetic interlayer exchange coupling. Therefore we exclude this type of interlayer exchange coupling mechanism for our system. For II–VI semiconductor structures the interlayer exchange coupling was explained by interaction via shallow donor impurities, which have, however, never been detected for PbS.^{26,27} A potential mechanism for interlayer exchange coupling would be a Bloembergen-Rowland-type mechanism, where the exchange interaction is mediated via virtual excitations in the PbS spacer. However, this mechanism leads to a ferromagnetic interlayer exchange coupling,²⁵ contrary to the observed antiferromagnetic coupling.

The observed temperature dependence of the interlayer exchange coupling constant can at least be qualitatively understood under the assumption that the coupling is determined by the changes in the band structure of the full EuS/PbS/EuS heterostructure induced by the exchange splitting of the *d*-type bands of EuS.³⁷ In a simple one-electron image the energy of the states inside a quantum well depends on the barrier height, and one therefore expects that the total free energy will depend on the exchange splitting in EuS. Thus, as the interlayer exchange coupling energy is determined by the difference in the total free energy between the parallel and the antiparallel configuration of the EuS magnetizations, it is expected to depend on the exchange splitting of the *d*-like bands in the EuS. Since the exchange splitting in EuS is approximately proportional to the magnetization, the interlayer exchange coupling energy should also depend on magnetization via the exchange splitting of the bands.³⁸ A recent theoretical study following this line of rea-

soning indeed shows a tendency for an antiferromagnetic interlayer exchange coupling, but only for larger PbS spacer thicknesses or much higher carrier densities in the well than is the case for our trilayers.³⁹ When the splitting of all bands, including the valence band, is taken into account and realistic band structures are used, the correct sign of the exchange coupling energy is obtained, as shown by Blinowski and Kacman in their calculations.²⁹

IV. CONCLUSIONS

We investigated the antiferromagnetic interlayer exchange coupling in high quality epitaxial EuS/PbS/EuS trilayers, and its dependence on spacer thickness and temperature by means of SQUID magnetometry. For spacer thicknesses exceeding 2.5 monolayers (7.5 Å) we observe that the interlayer exchange coupling energy diminishes with increasing spacer layer thickness, in agreement with data obtained by neutron reflectometry measurements¹⁰ and the calculations by Blinowski and Kacman.²⁹ For thinner spacer layers the antiferromagnetic interlayer exchange coupling energy decreases again, an effect that we ascribe to pinholes in the spacer causing strong local ferromagnetic coupling. Furthermore, an important observation was that the interlayer exchange coupling energy exhibited a very strong dependence on temperature. The interlayer exchange coupling constant J_{exch} showed a clear power law dependence on magnetization, with an exponent that, at first sight, seems to depend on the EuS layer thickness. While no theoretical description is available that can be readily used to describe the finite temperature properties of our system, we conjecture, along the line of reasoning proposed by Blinowski and Kacman,²⁹ that the observed power law dependence stems from a dependence of the interlayer exchange coupling energy on the exchange splitting of the bands in the two EuS layers.

ACKNOWLEDGMENTS

This work is part of the Research Program of the Stichting voor Fundamenteel Onderzoek der Materie (FOM) which is financially supported by the Nederlandse Organisatie voor Wetenschappelijk Onderzoek (NWO). The work in Poland was supported by Project No. PBZ-KBN-044/P03/2001. The support of the European Community Program ICA1-CT-2000-70018 (Center of Excellence CELDIS) and the Office of Biological and Physical Sciences of NASA is greatly appreciated.

*Electronic address: c.j.p.smits@tue.nl

¹H. Ohno, *Science* **291**, 840 (2001).

²T. Dietl, *Semicond. Sci. Technol.* **17**, 377 (2002).

³G.A. Prinz, *Science* **282**, 1660 (1998).

⁴S. A. Wolf, D. D. Awschalom, R. A. Buhrman, J. M. Daughton, S. von Molnár, M. L. Roukes, A. Y. Chtchelkanova, and D. M. Treger, *Science* **294**, 1488 (2001).

⁵J. K. Furdyna, X. Liu, Y. Sasaki, S. J. Potashnik, and P. Schiffer,

J. Appl. Phys. **91**, 7490 (2002).

⁶J. Nogués and K. Schuller, *J. Magn. Magn. Mater.* **192**, 203 (1999).

⁷D. E. Bürgler, P. Grünberg, S. O. Demokritov, and M. T. Johnson, in *Handbook of Magnetic Materials*, edited by K. H. J. Buschow (Elsevier, Amsterdam, 2001), Vol. 13, Chap. 1.

⁸For a review, see, for instance, A. Fert and P. Bruno, in *Ultrathin Magnetic Structures*, edited by J. A. C. Bland and B. Heinrich

- (Springer, Berlin, 1994), Vol. 2, Chap. 2.
- ⁹P. Bruno, Phys. Rev. B **52**, 411 (1995).
- ¹⁰H. Kępa, J. Kutner-Pielaszek, J. Blinowski, A. Twardowski, C. F. Majkrzak, T. Story, P. Kacman, R. R. Gałazka, K. Ha, H. J. M. Swagten, and W. J. M. de Jonge, Europhys. Lett. **56**, 54 (2001).
- ¹¹T. Jungwirth, W. A. Atkinson, B. H. Lee, and A. H. MacDonald, Phys. Rev. B **59**, 9818 (1999).
- ¹²H. Kępa, G. Springholz, T. M. Giebultowicz, K. I. Goldman, C. F. Majkrzak, P. Kacman, J. Blinowski, S. Holl, H. Krenn, and G. Bauer, Phys. Rev. B **68**, 024419 (2003).
- ¹³J. J. Rhyne, J. Lin, J. K. Furdyna, and T. M. Giebultowicz, J. Magn. Magn. Mater. **177-181**, 1195 (1998).
- ¹⁴H. Kępa, C. F. Majkrzak, A. Yu. Sipatov, and T. M. Giebultowicz, Physica B **335**, 44 (2003).
- ¹⁵D. Chiba, N. Akiba, F. Matsukura, Y. Ohno, and H. Ohno, Appl. Phys. Lett. **77**, 1873 (2000).
- ¹⁶A. Stachow-Wójcik, T. Story, W. Dobrowolski, M. Arciszewska, R. R. Gałazka, M. W. Kreijveld, C. H. W. Swüste, H. J. M. Swagten, W. J. M. de Jonge, A. Twardowski, and A. Yu. Sipatov, Phys. Rev. B **60**, 15220 (1999).
- ¹⁷L. Kowalczyk, M. Chernyshova, T. Story, J. K. Ha, V. V. Volobuev, and A. Yu. Sipatov, Acta Phys. Pol. A **100**, 357 (2001).
- ¹⁸M. Chernyshova, L. Kowalczyk, A. Szczerbakow, T. Story, C. J. P. Smits, H. J. M. Swagten, C. H. W. Swüste, J. K. Ha, W. J. M. de Jonge, A. Yu. Sipatov, and V. V. Volobuev, J. Supercond. **16**, 213 (2003).
- ¹⁹For a review, see, e.g., A. Mauger and C. Godart, Phys. Rep. **141**, 51 (1986).
- ²⁰L. Esaki, P. J. Stiles, and S. von Molnar, Phys. Rev. Lett. **19**, 852 (1967).
- ²¹X. Hao, J. S. Moodera, and R. Meservey, Phys. Rev. B **42**, 8235 (1990).
- ²²R. Dornhaus, G. Nimtz, and B. Schlicht, *Narrow Gap Semiconductors* (Springer, Berlin, 1983).
- ²³P. Kacman, Semicond. Sci. Technol. **16**, R25 (2001).
- ²⁴N. Akiba, F. Matsukura, A. Shen, Y. Ohno, H. Ohno, A. Oiwa, S. Katsumoto, and Y. Iye, Appl. Phys. Lett. **73**, 2122 (1998).
- ²⁵V. K. Dugaev, V. I. Litvinov, W. Dobrowolski, and T. Story, Solid State Commun. **110**, 351 (1999).
- ²⁶P. Shevchenko, L. Świerkowski, and J. Oitmaa, J. Magn. Magn. Mater. **177-181**, 1168 (1998).
- ²⁷T. M. Rusin, Phys. Rev. B **58**, 2107 (1998).
- ²⁸H. Heinrich, *Lecture Notes in Physics* (Springer, Heidelberg, 1980), Vol. 133, p. 407.
- ²⁹J. Blinowski and P. Kacman, Phys. Rev. B **64**, 045302 (2001).
- ³⁰M. Chernyshova, E. Łusakowska, V. Domukhovski, K. Graszka, A. Szczerbakow, S. Wrotek, L. Kowalczyk, T. Story, C. J. P. Smits, H. J. M. Swagten, W. J. M. de Jonge, W. Palosz, A. Yu. Sipatov, and V. V. Volobuev, Acta Phys. Pol. A **102**, 609 (2002).
- ³¹I. V. Kolesnikov and A. Yu. Sipatov, Sov. Phys. Semicond. **23**, 598 (1989).
- ³²G. Kneer and W. Zinn, Z. Angew. Phys. **26**, 152 (1968).
- ³³E. C. Stoner and E. P. Wohlfarth, Nature (London) **160**, 650 (1947); E. C. Stoner and E. P. Wohlfarth, Philos. Trans. R. Soc. London, Ser. A **240**, 599 (1948).
- ³⁴The exact details of the fitting procedure will be described elsewhere.
- ³⁵P. Bruno, *Magnetische Schichtsysteme*, edited by P. H. Dederichs and P. Grünberg (Forschungszentrum, Jülich, 1999).
- ³⁶P. Bruno, J. Phys.: Condens. Matter **11**, 9403 (1999).
- ³⁷This line of reasoning is also the basis of the calculations by Binowski and Kacman, who actually take into account the exchange splitting of all bands in EuS, see Ref. 27.
- ³⁸P. Wachter, CRC Crit. Rev. Solid State Sci. **3**, 189 (1972).
- ³⁹V.V. Zorchenko, A. Yu. Sipatov, and V.V. Volobuev, Low Temp. Phys. **29**, 1208 (2003).